Supporting Information

Ultrathin Graphitic Carbon Nitride Nanosheet: A Novel Inhibitor of Metal-induced Amyloid Aggregation Associated with Alzheimer's Disease

Materials. Dicyandiamide was purchased from Sigma-Aldrich. Aβ40 was obtained from American peptide. All these reagents were used as received without further purification. Deionized water (18.2 MΩ cm) used for all experiments was obtained from a Milli-Q system (Millipore, Bedford, MA).

Apparatus and Characterization. The samples were characterized by X-ray powder diffraction (XRD) with a Japan Rigaku Dmax X-ray diffractometer equipped with graphite monochromatized high-intensity Cu-Kα radiation (λ=1.54178 Å). Fluorescence spectra were carried out on a JASCO FP-6500 spectrofluorometer. All spectra were recorded in a 1.0 cm path length cell. AFM measurements were performed using Nanoscope V multimode atomic force microscope (Veeco Instruments, USA). TEM images were recorded using a FEI TECNAI G2 20 high-resolution transmission electron microscope operating at 200 kV. X-ray photoelectron spectra (XPS) were acquired on an ESCALab220i-XL electron spectrometer from VG Scientific using 300W Al Kαas the excitation source. The binding energies obtained in the XPS spectral analysis were corrected for specimen charging by referencing C1s to 284.8 eV.

Preparation of bulk g-C_3N_4. The bulk g-C_3N_4 was prepared by thermal polycondensation of dicyandiamide. In a typical synthesis, 10 g dicyandiamide was

put into a crucible with a cover and calcined at settled temperatures for 4 h in a muffle furnace, using a heating rate of 2.3 ℃ min^{-1}. The sample was then allowed to cool to room temperature before removal from the furnace. Yellow products were obtained after this polycondensation step.

Preparation of ultrathin g-C_3N_4 nanosheets. The ultrathin g-C_3N_4 nanosheets were obtained by liquid exfoliating of as-prepared bulk g-C_3N_4 in water. In detail, 100 mg of bulk g-C_3N_4 powder dispersed in 100 mL water, and then ultrasound for about 16 hours. The initial formed suspension was then centrifuged at about 5000 rmp to remove the residual unexfoliated g-C_3N_4 nanoparticles and large-area nanosheets before used for further study.

Aβ Preparation. Aβ40 (lot no. U10012) was purchased from American Peptide and prepared as previously described. Briefly, the powered Aβ peptide was first dissolved in 1,1,1,3,3,3-hexafluoro-2-propanol (HFIP) at the concentration of 1 mg/ml. The solution was shaking at 4 °C for 2 hours in a sealed vial for further dissolution and was then stored at -20 °C as a stock solution. Before use, the solvent HFIP was removed by evaporation under a gentle stream of nitrogen and peptide was dissolved in water. Cu^{2+} induced aggregation of Aβ40 was accomplished by mixing an aliquot of the peptides and $CuCl_2$ at a molar ratio of 1:1 into 10 mM HEPES (150 mM NaCl, pH 6.6) at 37 °C for 24 h. For inhibition experiment, Aβ1-40 peptides and Cu^{2+} were aged with or without g-C_3N_4. While for the disaggregation experiment, the sample of aged Aβ40-Cu^{2+} was mixed with g-C_3N_4, which followed by further incubation of 4h.

Native Polyacrylamide Gel Electrophoresis. Native polyacrylamide gel

electrophoresis (PAGE) was carried out using a 12% gel. Gels were run in a Tris/Tricine system after which the gels were silver-stained.

Transmission Electron Microscopy. Samples (10 μL) were spotted onto carbon-coated copper grids for 30 min. The grids were blotted with filter paper to remove excess buffer and the sample was stained with 1.5% (w/v) phosphotungstic acid (pH 7.4). Grids were blotted again and air-dried before analysis on a transmission electron microscope, operating with a voltage of 100 kV.

Atomic Force Microscopy. AFM measurements were performed using a Nanoscope V multimode atomic force microscope (Veeco Instruments, USA). Samples for AFM images were diluted with deionized H_2O to yield a final concentration of 1×10^{-6} M. The sample (20 μL) was then applied onto freshly cleaved muscovite mica and allowed to dry. Tapping mode was used to acquire the images under ambient conditions.

Intracellular determination of ROS. The generation of reactive oxygen radicals was monitored using 2′, 7′-dichlorofluorescein diacetate (DCFH-DA). This dye is a nonfluorescent compound which readily diffuses into cells and reacts with intracellular free radicals. The product, dichlorofluorescein (DCF), is a fluorophor. The DCF fluorescence intensity correlates with the amount of intracellular reactive oxygen radicals. To perform the test, DCFH-DA solution (20 μM) was added to the cells, and the mixture was incubated at 37 °C for 1 h. The cells were then washed twice with PBS and finally, the fluorescence intensity was monitored on a fluorescence spectrofluorometer with excitation and emission wavelengths of 488 and

525 nm, respectively.

Cell Toxicity Assays. PC12 cells (rat pheochromocytoma, American Type Culture Collection) were cultured in DMDM (Gibco BRL) medium supplemented with 5% fetal bovine serum (FBS), 10% horse serum (HS) in a 5% CO_2 humidified environment at 37 °C. Prior to differentiation of PC12 cell, a well plate was coated with collagen type I (0.5 mg/mL) overnight. PC12 was seeded at a density of 5000 cells/cm^2 for MTT (3-(4,5-dimethylthiazol-2-yl)-2,5-diphenyltetrazolium bromide, Sigma-Aldrich) assay to minimize contact inhibition of neuritogenesis and incubated for 7 days in serum-reduced media (1% HS and 0.5% FBS) supplemented with 50 ng/mL NGF. After the cell differentiated, Aβ40 (5 μM), $CuCl_2$ (5 μM) and chelator were added. 48 hours later, the cells were treated with 10 μL MTT (5 mg/mL in PBS) for 4 h at 37 °C and then were lysed in DMSO for 10 min at room temperature in the dark. Absorbance values of formazan were determined at 570 nm with a Bio-Rad model-680 microplate reader.

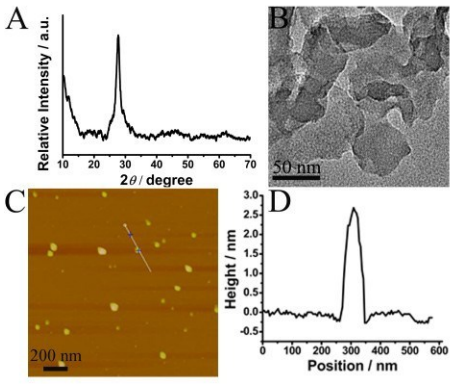

Figure S1 (A) X-ray diffraction pattern of g-C_3N_4 nanosheets. (B) TEM images of the as-synthesized g-C_3N_4 nanosheets. (C) AFM image of thus obtained g-C_3N_4

nanosheets and (D) The height of g-C_3N_4.

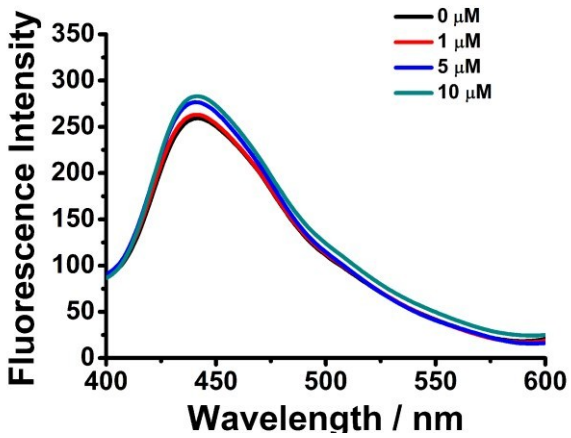

Figure S2 The effect of Aβ40 on the fluorescence of g-C_3N_4 nanosheet.

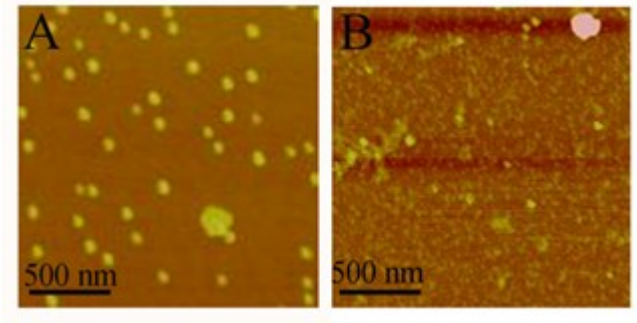

Figure S3 Determination of the inhibition effects of g-C_3N_4 nanosheets on the Cu^{2+}-induced formation of Aβ40 aggregates by AFM: (A) Aβ40-Cu^{2+} complex, (B) Aβ40-Cu^{2+} complex with g-C_3N_4. [Aβ40] = 10 μM, [Cu^{2+}] = 10 μM, [g-C_3N_4] = 20 $\mu g ml^{-1}$. Buffer: 10 mM HEPES, 150 mM NaCl, pH 6.6.

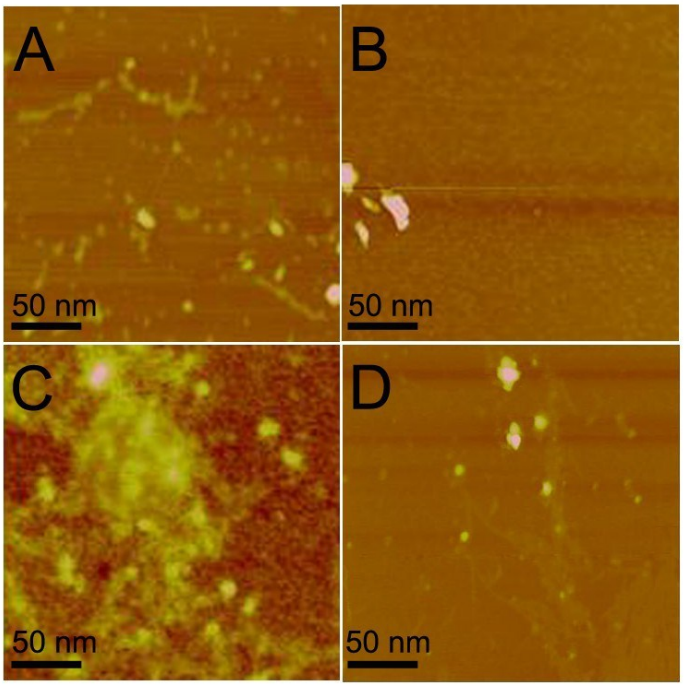

Figure S4 Determination of the inhibition effects of g-C_3N_4 nanosheets on the Cu^{2+}-induced formation of Aβ40 aggregates at different Cu^{2+}:Aβ40 ratios: (A) Aβ40-Cu^{2+} complex at a 0.1:1 molar Cu^{2+}:Aβ40 ratio, (B) Aβ40-Cu^{2+} complex with g-C_3N_4 at a 0.1:1 molar Cu^{2+}:Aβ40 ratio. (C) Aβ40-Cu^{2+} complex at a 5:1 molar Cu^{2+}:Aβ40 ratio, (D) Aβ40-Cu^{2+} complex with g-C_3N_4 at a 5:1 molar Cu^{2+}:Aβ40 ratio. [Aβ40] = 10 μM, [g-C_3N_4] = 20 $\mu g ml^{-1}$. Buffer: 10 mM HEPES, 150 mM NaCl, pH 6.6. At a 0.1:1 molar Cu^{2+}:Aβ40 ratio, spherical aggregates and a few fibrillar structures were observed in Aβ-Cu^{2+} complex sample under our incubation condition. However, in the presence of g-C_3N_4 nanosheets, the fibrillar structures and spherical aggregates almost disappeared, indicating the g-C_3N_4 nanosheets could chelate the Cu^{2+} ions and inhibit Cu^{2+}-induced aggregation of Aβ40 at subequimolar Cu^{2+}:Aβ40 ratio. On the other hand, at a 5:1 molar Cu^{2+}:Aβ40 ratio, some spherical aggregates were found in Aβ-Cu^{2+} complex sample. Upon co-incubation with g-C_3N_4 nanosheets,

Aβ-Cu^{2+} complexes were promoted to form fibrillar structures. The detailed mechanism behind the inhibition effects will be discussed in our future work.

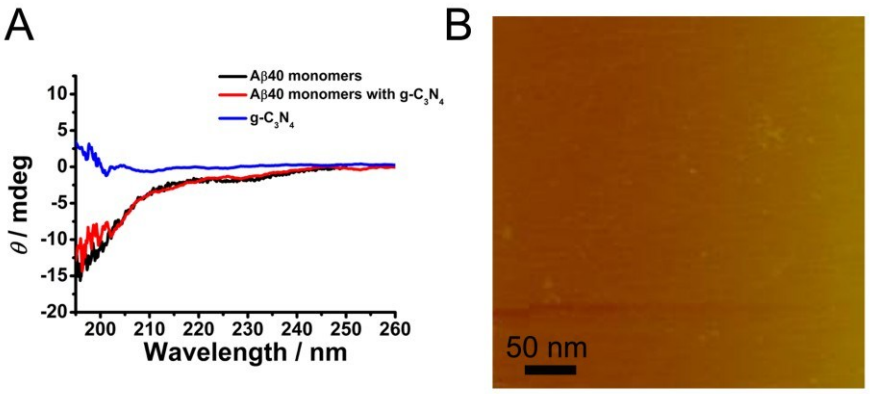

Figure S5 (A) Circular dichroism spectra of Aβ40 at the start of the experiment with or without g-C_3N_4 nanosheets. (B) AFM image of Aβ40 at the start of the experiment.

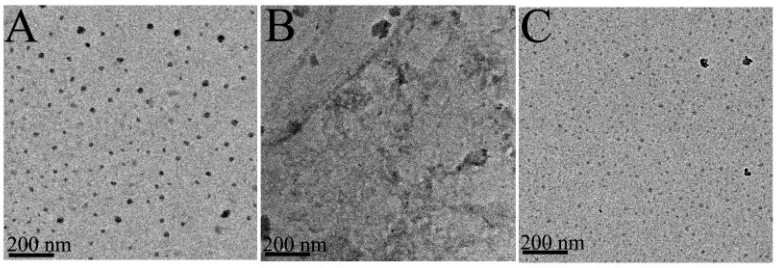

Figure S6 Disassociation of Aβ40-Cu^{2+} aggregates by g-C_3N_4 nanosheets. TEM images of samples of (A) Aβ40-Cu^{2+} aggregates, (B) the performed Aβ40-Cu^{2+} aggregates treated with g-C_3N_4 for 4hs, (C) the performed Aβ40-Cu^{2+} aggregates treated with CQ for 4hs. [Aβ40] = 10 μM, [Cu^{2+}] = 10 μM, [g-C_3N_4] = 20 μgml^{-1}, [CQ] = 20 μgml^{-1}.

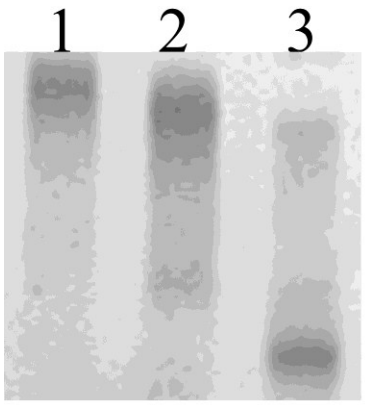

Figure S7 Determination of the disassociation effects of g-C_3N_4 on the Cu^{2+}-induced formation of Aβ40 aggregates by native-PAGE: (1) Aβ40-Cu^{2+} complex, (2) the performed Aβ40-Cu^{2+} aggregates treated with 2 μgml^{-1} g-C_3N_4, (3) the performed Aβ0-Cu^{2+} aggregates treated with 20 μgml^{-1} g-C_3N_4, [Aβ40] = 10 μM, [Cu^{2+}] = 10 μM. Buffer: 10 mM HEPES, 150 mM NaCl, pH 6.6.

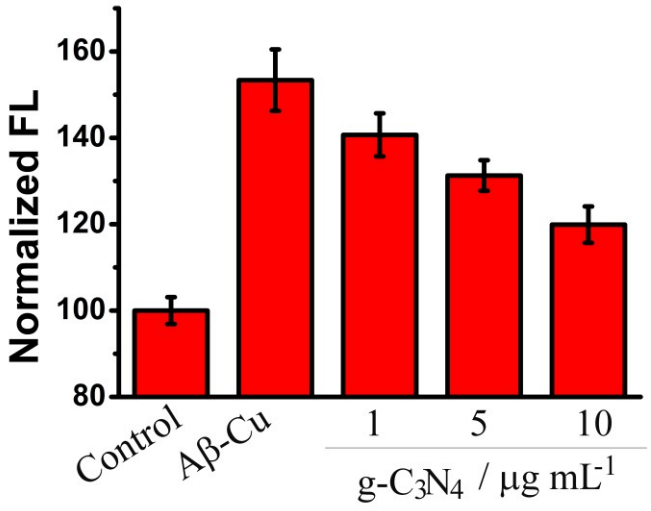

Figure S8 Cells were treated with aged Aβ40-Cu^{2+} disassociated with or without g-C_3N_4 nanosheets and ROS generation inside the cells after 24 h was measured using DCF fluorescence. Data represents mean ± SEM of at least three different experiments. Control: Aβ40-Cu^{2+}-untreated cells, [Aβ40] = 5 μM, [Cu^{2+}] = 5 μM.

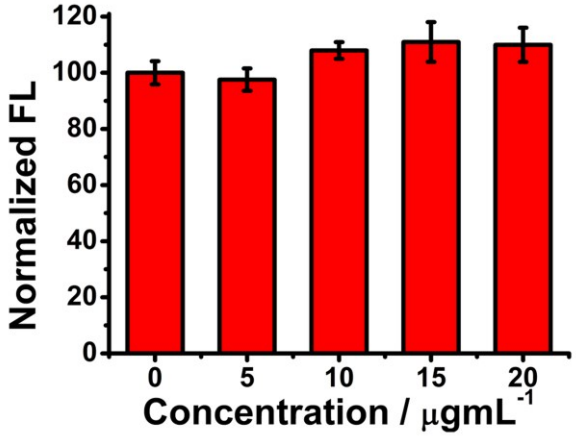

Figure S9 Effects of the g-C_3N_4 nanosheets on the production of ROS in PC12 cells.

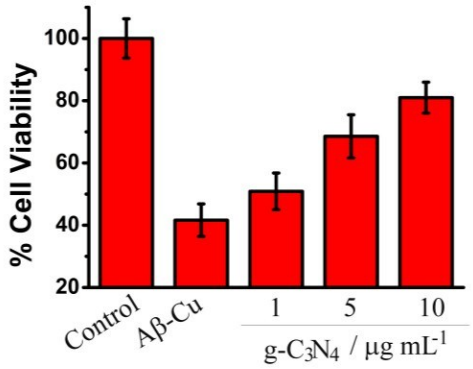

Figure S10 Protection effects of g-C_3N_4 nanosheets on Aβ40-Cu^{2+}-induced cytotoxicity of differentiated PC12 cells in the disaggregtion study. Cell viability was determined using the MTT method and data points shown are the mean values ±SEM from three independent experiments. Control: Aβ40-Cu^{2+}-untreated cells, [Aβ40] =5 μM, [Cu^{2+}] = 5 μM.

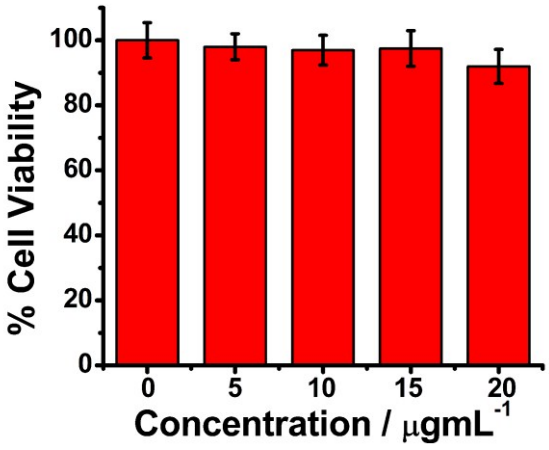

Figure S11 Effects of the g-C_3N_4 nanosheets on differentiated PC12 cell viability determined by MTT method.